Available online at www.sciencedirect.com
SCIENCE DIRECT
Developmental Biology 289 (2006) 17 – 29
DEVELOPMENTAL BIOLOGY
www.elsevier.com/locate/ydbio

Calcineurin function is required for myofilament formation and troponin I isoform transition in *Drosophila* indirect flight muscle

Kathleen M. Gajewski *, Jianbo Wang, Robert A. Schulz

Department of Biochemistry and Molecular Biology, The University of Texas M.D. Anderson Cancer Center, 1515 Holcombe Boulevard, Houston, TX 77030, USA

Received for publication 8 July 2005, revised 15 September 2005, accepted 21 September 2005
Available online 17 November 2005

Abstract

Mutations in the *Drosophila* calcineurin B2 gene cause the collapse of indirect flight muscles during mid stages of pupal development. Examination of cell fate-specific markers indicates that unlike mutations in genes such as vestigial, calcineurin B2 does not cause a shift in cell fate from indirect flight muscle to direct flight muscle. Genetic and molecular analyses indicate a severe reduction of myosin heavy chain gene expression in calcineurin B2 mutants, which accounts at least in part for the muscle collapse. Myofibrils in calcineurin B2 mutants display a variety of phenotypes, ranging from normal to a lack of sarcomeric structure. Calcineurin B2 also plays a role in the transition to an adult-specific isoform of troponin I during the late pupal stages, although the incompleteness of this transition in calcineurin B2 mutants does not contribute to the phenotype of muscle collapse. Together, these findings suggest a molecular basis for the indirect flight muscle hypercontractility phenotype observed in flies mutant for *Drosophila* calcineurin B2.

Keywords: Calcineurin; *Drosophila*; Hypercontraction; Indirect flight muscle; Myosin heavy chain; Troponin I

Introduction

The diversity of muscle structural isoforms allows for the generation of muscle fibers with different physiological properties. The presence of various isoforms can cause differences in the speed and force of muscle contraction, the consumption of ATP, calcium sensitivity, and even the structure of the myofibril. One well-characterized example is that of the fast-twitch and slow-twitch fiber types found in vertebrate skeletal muscle. Unique structural isoforms have also been documented in the mandibular, eye, ear, and laryngeal muscles of various vertebrate species (reviewed in Schiaffino and Reggiani, 1996). The indirect flight muscles (IFM) of insects contain unique structural isoforms of molecules such as myosin heavy chain (mhc), troponin I (Tn I), actin, and myosin light chain 1 (reviewed in Bernstein et al., 1993), which give these muscles characteristics such as the ability to contract faster than incoming nerve impulses (asynchronous contraction), and their properties of stretch activation (Peckham et al., 1990). There are two basic types of strategies to insure expression of specific isoforms: (1) multigene families and (2) alternative splicing of a single gene. Examples of each can be found in both vertebrates and invertebrates.

The serine-threonine phosphatase calcineurin plays a role in controlling several important processes in skeletal muscle, including fiber type switching and differentiation (reviewed in Schulz and Yutzey, 2004). The control of fiber type switching is affected at the transcriptional level. It is known that cyclosporine A, an inhibitor of calcineurin (Liu et al., 1991), causes an increase in amounts of fast twitch fiber at the expense of slow twitch fiber (Chin et al., 1998; Dunn et al., 1999). Extended periods of tonic nerve activity cause a sustained increase in the calcium concentration inside muscle cells, a condition necessary for calcineurin activation. Activated calcineurin increased transcription from reporter constructs with enhancer regions from slow fiber genes such as *myoglobin* and *Tn I*, slow in cultured skeletal myotubes, but had no effect on the fast fiber *muscle creatine kinase* control region (Chin et al., 1998). These slow fiber-specific control regions contain sequences that are bound by the transcription factor nuclear factor of activated T-cells (NFAT). Calcineurin controls NFAT activity by dephosphorylation, which allows NFAT to enter the

* Corresponding author. Fax: +1 713 834 6291.
E-mail address: kwgajews@mdanderson.org (K.M. Gajewski).

0012-1606/$ - see front matter © 2005 Elsevier Inc. All rights reserved.
doi:10.1016/j.ydbio.2005.09.039

nucleus and activate its target genes (Flanagan et al., 1991; Liu et al., 1991). The slow fiber control regions also require Sp1 and Mef2 binding for full activation (Chin et al., 1998). Calcineurin influences the ability of Mef2 to act as a transcriptional activator by relieving histone deacetylase-mediated repression of target gene activation by Mef2 (Zhang et al., 2002) and possibly by direct dephosphorylation of Mef2 (Wu et al., 2001). During skeletal muscle differentiation, calcineurin is needed for complete activation of Mef2 and the muscle regulatory factor MyoD. Whether calcineurin directly activates MyoD expression is not known, but an indirect effect has been shown. Calcineurin negatively regulates Egr-1, which is an activator of the MyoD inhibitors Id1 and Id3 (Friday et al., 2003). Thus, calcineurin is strongly implicated to play an important role in multiple aspects of muscle development.

The system of *Drosophila* IFM consists of six centrally located pairs of dorsal longitudinal muscles (DLM) and two sets of seven laterally located dorsoventral muscles (DVM). These groups of muscles power the wings by compression of the thorax, and act in opposition to each other. The IFM originate from a subset of the adepithelial cells of the wing imaginal discs. DLM development follows a unique pattern. Three pairs of larval oblique muscles (LOM) survive the wave of histolysis in the early pupal stages. A portion of the adepithelial cells migrate from the discs and begin to fuse to them at 8 h after puparium formation (APF). The fusion continues until about 30 h APF (Fernandez et al., 1991). Each of these LOM templates will split longitudinally between 14 and 20 h APF, giving rise to six developing DLMs in each hemisegment. In contrast, the DVM use no preserved larval templates; the adepithelial cells fuse de novo to form the muscle fibers (Fernandez et al., 1991; Rivlin et al., 2000).

Recent studies have uncovered a requirement for calcineurin function in the proper formation of *Drosophila* IFM (Gajewski et al., 2003). *canB2[EP(2)0774]* is a well-characterized allele of the *calcineurin B2 (canB2)* gene, one of the two *Drosophila* versions of the regulatory B subunit. It is a semi-lethal, with frequent adult homozygous escapers that display a held out wings phenotype. This is caused by a collapse of IFMs during the later stages of pupal development. Examination of the muscle structure in adult homozygotes revealed a range of IFM defects. In the mildest cases, half of the six pairs of DLM had collapsed to the back of the thorax; in the most severe cases, all the DLM and the DVM collapse. *canB2* transcripts are detected in the developing IFM in the pupal stages, along with at least one version of the catalytic *calcineurin A* gene (*Pp2B-14D*). In contrast, transcripts of *calcineurin B* (*canB*), the other version of the regulatory subunit, are not detectable by in situ hybridization in this tissue. Both *canB* genes and *Pp2B-14D* are expressed prominently in the nervous system during embryonic stages and appear to play no role in embryonic muscle development (Gajewski et al., 2003).

The exact role of calcineurin in *Drosophila* IFM development is not yet known. The early stages of DLM formation such as preservation of the LOM as templates, template splitting, myoblast fusion, and initial elongation of the muscle fibers appear to be normal in *canB2* mutants (Gajewski et al., 2003). The collapse of the IFM during later pupal development is reminiscent of some mutations in the *mhc* and *Tn I* genes (Beall and Fyrberg, 1991; Barbas et al., 1993; Kronert et al., 1995, 1999). The flight muscles of these flies display a hypercontracted phenotype, which is defined as a disruption of muscle structure due to an absence of regulation of the interaction between thick and thin filaments (Nongthomba et al., 2004). Alternatively, a switch in precursor cell fate is a potential cause of the *canB2* phenotype. This process happens late in the 3rd instar larval stage, when cells that will form flight muscles are adepithelial cells associated with the wing imaginal discs. The genes *vestigial* (*vg*) and *cut* (*ct*) play a critical role in this process. Adepithelial cells that express *vg* and low levels of *ct* will play a role in the formation of the IFM. The remaining cells, which express high levels of *ct* and no *vg*, contribute to the direct flight muscles (DFM; Sudarsan et al., 2001). One of the functions of *vg* in the cells fated to form IFM is to prevent the expression of *apterous* (*ap*), which helps specify a DFM fate. Lack of *vg* expression in the IFM causes ectopic expression of *ap*, a conversion to a DFM cell fate, and apoptosis and degeneration of the IFM tissue (Bernard et al., 2003).

In this paper, we further characterize the muscle collapse phenotype of *canB2* mutants. We show that unlike *vg* mutants, the IFM of *canB2* mutants do not undergo a shift in cell fate to the DFM state. We also demonstrate that expression of an important structural protein gene, *mhc*, is greatly reduced in *canB2* mutant IFMs. Our results also suggest a previously uncharacterized role for calcineurin, that being the control of alternative splicing of *Tn I* RNAs during a late pupal stage.

Materials and methods

Fly strains

The *88Factin-GFP* fly stock was obtained from S. Bernstein (San Diego State University, San Diego), the *fli I[3]* and *Mhc[5]/CyO* stocks from the Bloomington Stock Center (Indiana University, Bloomington) and *gD1142.1-lacZ* flies from D. Standiford (University of Pennsylvania School of Medicine, Philadelphia). The *canB2[EP(2)0774], mhc-GFP/CyO GFP-Actin* strain has been described previously (Gajewski et al., 2003). The *canB2[EP(2)0774], 88Factin-GFP / CyO GFP-Actin* and *gD1142.1 canB2[EP(2)0774], MHC-GFP/CyO GFP-Actin* fly strains were made with standard recombination techniques. Flies were raised at 22°C on standard media. Live animals expressing GFP were photographed as described previously (Gajewski et al., 2003).

Immunohistochemical staining of paraffin sections

Embedding of adult thoraces and preparation of paraffin sections was done as described by Lyons et al. (1990). Slides were stored at −20°C until used for immunostaining. The slides were dewaxed in 3 changes of Histoclear (National Diagnostics, Atlanta GA), then rehydrated through a series of two washes of 100% ethanol, one wash each of 95% and 70% ethanol, one wash of PBS, and two washes in distilled water. This was followed by microwave treatment of the slides in 10 mM sodium citrate (pH 6.0) for 7 min at high power (~95°C) and 15 min at low power (~85°C). After the slides were allowed to cool for 30 min, they were washed twice in distilled water, then soaked in 3% hydrogen peroxide in methanol for 30 min. The slides were then washed twice in distilled water, once in TBST buffer (0.1 M Tris pH 7.5, 0.15 M NaCl, 0.1% Tween-20), and blocked for at least 1 h at room temperature in blocking solution (10% normal goat serum in TBST). The primary antibody (anti-β galactosidase,

Promega, Madison, WI) was diluted 1:1000 in blocking solution, and the slides incubated overnight at 4°C with coverslips in a humid chamber. The next day the slides were washed three times, 10 min each in TBST, then incubated for 30 min at room temperature with secondary antibody (biotin-conjugated horse anti-mouse, Vector, Burlingame, CA) diluted 1:1000 in blocking solution. The slides were washed in TBST, incubated for 30 min at room temperature in peroxidase-conjugated streptavidin in blocking solution, and washed again in TBST. The Vectastain DAB kit (Vector) was used for staining the slides, and the reaction monitored under a microscope. The staining reaction was stopped by washing in distilled water, and the slides were dehydrated through an ethanol series and several washes in Histoclear, then mounted in Permount (Fisher, Pittsburgh, PA). Images of stained sections were captured with a Zeiss Axioplan 2 microscope and digital camera using AXIOVISION V3.1 software.

Genetic tests

To produce flies transheterozygous for *canB2[EP(2)0774]* and *Mhc[5]*, flies with these mutations over a *CyO GFP-Actin* balancer were crossed, and offspring lacking the balancer were selected as larvae. A *fli[3]; canB2[EP(2)0774]/CyO GFP-Actin* stock was made with standard genetic techniques, and double homozygotes selected as larvae for lack of the *CyO GFP-Actin* balancer. Thoraces were prepared for sectioning as described above. Sections were photographed under fluorescent light using a GFP filter with a Zeiss Axioplan 2 microscope using AXIOVISION V.3.1 software.

Freeze drying of flies

88Factin-GFP and *canB2[EP(2)0774], 88Factin-GFP* flies were dried in acetone as described by Fujita et al. (1987; Method B). IFM fibers or whole abdomens dissected from freeze-dried flies were stored in Eppendorf tubes at −70°C until used for RNA isolation and reverse transcriptase-PCR (RT-PCR). Pupae at the start of the second DLM elongation (referred to as "stage 1" below) and completion of the second DLM elongation ("stage 2") stages were collected by monitoring the muscle development of pools of wild type and mutant animals using the *88Factin-GFP* marker, and freeze drying animals of the appropriate stage. To collect pupae at the time point of muscle collapse in the *canB2* mutants ("stage 3"), white prepupae (0 h APF) of both wild type and *canB2* mutant genotypes (carrying the *88Factin-GFP* marker) were collected at the same time, monitored periodically under fluorescent light, and freeze dried when the mutant IFM began their collapse.

RT-PCR

Freeze dried fly tissues were homogenized in liquid nitrogen, then resuspended in 100 μl DEPC treated water with 20 μg yeast tRNA (as a carrier). Total RNA was extracted using 0.5 ml TRIzol (Invitrogen, Carlsbad CA), following the standard protocol for isolation of RNA from less than 10 mg of tissue. Reverse transcription to make cDNA was done with the SuperScript First-Strand Synthesis Kit (Invitrogen). The following primers were used for PCR reactions: MHCex2i-s (5′-GACTCGAAGAAGTCTTGCTG-3′), MHCex11e-as (5′-CAAGCACTTTCCGGCAGCATTC-3′), MHCex11a.1-as (5′-CGAGGTCCTTAATGCCACGG-3′), MHCex11b-as (5′-CCAAAATGATGGATCCACAC-3′), MHCex11c-as (5′-TCTTGGGATCCTCAATACCC-3′), MHCex11d-as (5′-AACGGTACTGATCTTCGGGC-3′), MHCex6-S (5′-TGTCATCTCCCAGCAGTCC-3′), MHCex12.2-as (5′-TGCGGCTGACGTTGAGGAGG-3′), wupAex2-s (5′-CAAATCAAAATGGCTGATGATGAG-3′), wupAex5-as (5′-GCTGGCATCGCTGAGATTCC-3′), 88F.2-s (5′-CGTTGACCTAAAAGGATAAACAACTGCC-3′), 88F.2-as (5′-TTGCTGCCTTTGAAGAGCTTTCGCG-3′). PCR products to be sequenced were cloned using the TOPO TA Cloning kit (Invitrogen) and DNA for sequencing prepared with the Qiaprep Spin Miniprep kit (Qiagen, Valencia CA). All PCR reactions used 30 cycles unless otherwise indicated.

Electron microscopy of IFM

Flight muscles from five wild type adults, five *canB2[EP(2)0774]* adults and four *canB2[EP(2)0774], 88Factin-GFP* mid-stage pupae were fixed and dissected as described in Beall and Fyrberg (1991). The muscles were postfixed with 1% buffered osmium tetroxide for 1 h, dehydrated in increasing concentrations of ethanol, infiltrated, and embedded in Epon812/dodecenyl-succinic anhydride/araldite. The samples were polymerized in a 60°C oven for 2 days. Ultrathin sections were cut in a Leica Ultracut microtome (Leica, Deerfield, IL), stained with uranyl acetate and lead citrate in a Leica EM strainer, and examined in a JEM 1010 transmission electron microscope (JEOL, USA, Inc., Peabody, MA) at an accelerating voltage of 80 kV. Digital images were obtained using AMT Imaging System (Advanced Microscopy Techniques Corp., Danvers, MA).

Results

Normal expression of IFM and DFM markers in a canB2 mutant background

Previous studies of *vg[null]*, a mutation that causes adepithelial cells fated to form IFM to shift to a DFM fate, demonstrated a failure to express an IFM-specific marker, *88Factin-GFP*, in the developing IFM of mutant flies (Bernard et al., 2003). To test if the IFM of *canB2* mutants had experienced a similar fate shift, we examined the expression of this marker in a *canB2* mutant background. The *88Factin-GFP* construct mimics the expression pattern of the native *88F actin* gene, expressed in the IFM of the pupal/adult thorax. In the wild type control, expression can be observed at the start of second DLM elongation (and the beginning of myofibrillogenesis) (Fig. 1A), at the completion of the second IFM elongation (Fig. 1B), and in later stages (after 90 h APF) (Fig. 1C). Expression in a *canB2[EP(2)0774]* mutant background resembles that of wild type at the first two time points (Figs. 1D and E). Although the IFM of the *canB2* mutants have collapsed well before the 90-h time point, there is no discernable alteration in expression of the *88Factin-GFP* reporter construct (Fig. 1F). In contrast, no GFP expression from this construct was reported in a *vg[null]* background (Bernard et al., 2003).

vg[null] mutants also showed ectopic expression of DFM markers in the IFM, a direct indication of a fate change (Bernard et al., 2003). To test for this in *canB2* mutants, we used the *gD1142.1-lacZ* construct, a marker for expression of the myosin rod protein. In the adult thorax, this reporter is expressed strongly in three pairs of DFM (muscles 49, 53, and 54) (Standiford et al., 1997b). β-galactosidase staining of whole thoraces from *canB2* mutants carrying this marker showed a pattern of three stained DFM on each side, similar to the wild type pattern (data not shown). Horizontal sections of both wild type (Fig. 1G) and mutant (Fig. 1H) animals stained with an anti β-galactosidase antibody showed the same pattern of expression in a subset of DFM and no expression in other DFM or the IFM. Therefore, the *canB2* mutants express an IFM- and a DFM-specific marker in the correct locations, which is indicative of normal specification of muscle cell fate.

The canB2 IFM collapse phenotype is suppressed by flightless I[3]

Since the results with IFM- and DFM-specific markers ruled out a change in cell fate, hypercontraction remained a likely explanation for the *canB2* phenotype. To test this possibility,

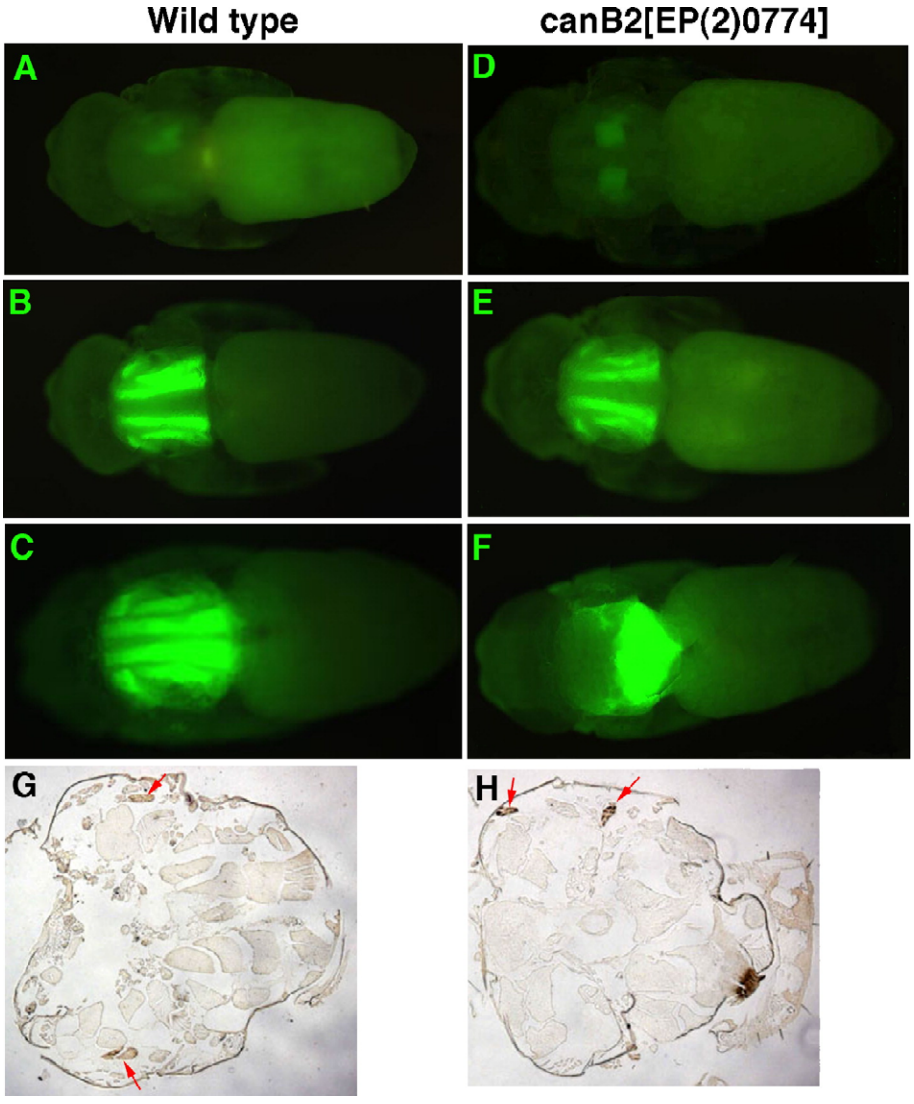

Fig. 1. *canB2* mutants show normal expression of an IFM and a DFM-specific marker. (A–C) Wild type animals with the *88Factin-GFP* reporter, (D–F) *canB2[EP(2)0774]* animals with the *88Factin-GFP* reporter, (A and D) pupae at about 44 h, at the beginning of myofibrillogenesis, (B and E) pupae at the completion of the second IFM elongation, at roughly 60–66 h, (C and F) pupae older than 90 h. (G) Horizontal section of a wild type fly carrying the *gD1142.1-lacZ* reporter, stained with an antibody against β-galactosidase. A pair of stained DFM are indicated by the red arrows. (H) Horizontal section of a homozygous *canB2[EP(2)0774]* fly carrying the *gD1142.1-lacZ* reporter, stained with an antibody against β-galactosidase. The section is at an angle, so that two DFM on only one side are visible (red arrows).

we examined the effects of reduced *flightless I (fli I)* function in combination with the *canB2* mutation. *fli* is a member of the gelsolin protein family, involved in the capping, severing, and bundling of actin filaments (de Couet et al., 1995). Strong *fli* I alleles are lethal in early embryogenesis, but weaker alleles, such as *fli I[3]*, are viable but flightless. Mutant muscles have severely disrupted Z-bands and peripheral fraying of the myofibrils (Miklos and De Couet, 1990), which could be expected to compromise their ability to contract. One copy of *fli I[3]* in a *canB2* mutant background had no effect on the IFM collapse phenotype (data not shown). However, flies doubly homozygous for both *fli I[3]* and *canB2[EP(2)0774]* displayed a strong suppression of muscle collapse. Examination of the *mhc-GFP* marker in live animals revealed a distinct difference between the *canB2* mutants and the double *fli I[3]; canB2[EP(2)0774]* mutants. Complete collapse of all the DLM is common in *canB2* homozyotes, and occurs in the mid pupal stage, before pigment appears in the pupal eye (Fig. 2A). The double mutants clearly showed uncollapsed DLM in the later stages of pupal development (Fig. 2B).

Cross sectioning of these flies provided a clearer picture of the suppression of the *canB2* phenotype (Figs. 2C–E). To quantitate the differences between the two genotypes, we counted the number of DLM in the anterior portion of the thoraces; DLM were scored because they are the most severely affected by reduced calcineurin function, and are easier to score than DVM in cross sections. The majority of the DLM failed to collapse in all double mutants examined, with no less than seven (Fig. 2C) and as many as all twelve present (Fig. 2D). However, these muscles were often not wild type in appearance. Holes were commonly seen in the cytoplasm (Fig. 2C, arrowhead), as were DLM fibers smaller than normal (Fig. 2C, arrow). In

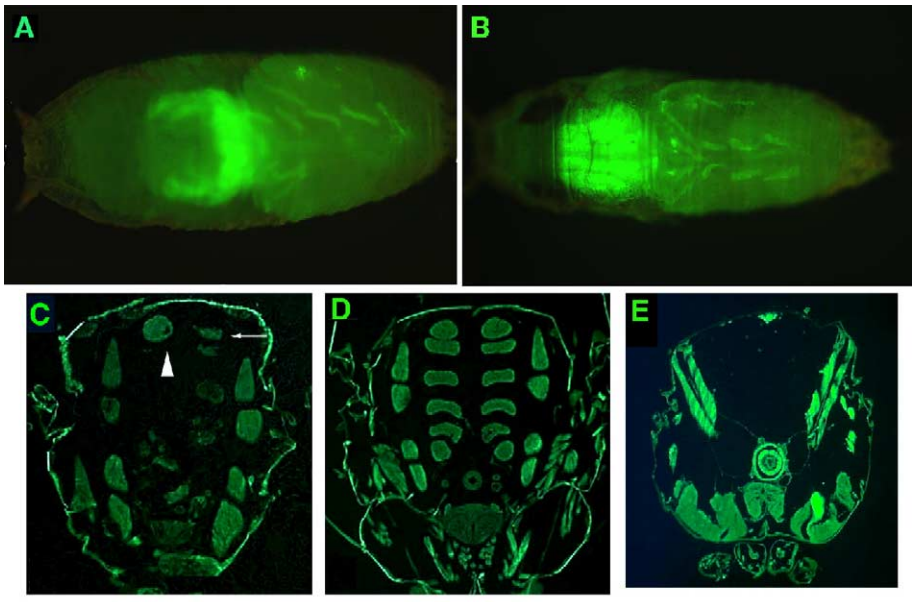

F

	fli l[3] / fli l[3] ; canB2[EP(2)0774] / canB2[EP(2)0774]	canB2[EP(2)0774] / canB2[EP(2)0774]
Average number of DLM (n=15)	8.4	1.0

Fig. 2. The *flightless I[3]* mutation can suppress the collapse of *canB2* mutant IFM. (A) Dorsal view of a mid-stage *canB2[EP(2)0774]* homozygous pupa with the *mhc-GFP* reporter, showing a collapse of all IFM. (B) Dorsal view of a late *fli I[3]; canB2[EP(2)0774]* double homozygous pupa with the *mhc-GFP* reporter, showing a number of IFM have not collapsed. Note this pupa has full pigmentation of the eyes. (C) Cross section through the anterior thorax of a *fli I[3]; canB2 [EP(2)0774]* double homozygous fly, showing a weak suppression of the muscle collapse phenotype. (D) Cross section through the anterior thorax of a *fli I[3]; canB2 [EP(2)0774]* double homozygous fly, showing a complete suppression of the muscle collapse phenotype. (E) Cross section the thorax of a homozygous *canB2 [EP(2)0774]* fly showing the most severe phenotype, where all the IFM have collapsed. (F) Average numbers of DLMs observed in the anterior thoraces of double (8.4) and single (1.0) mutant flies (the wild type average is 12.0).

contrast, over 70% of the *canB2* mutants had complete collapse of all DLM (Fig. 2E), and no animal had more than 7 uncollapsed DLM. In the double mutants, the average number of uncollapsed DLM observed was 8.4 per thorax, while *canB2* single mutants averaged 1 per thorax (Fig. 2F), (Student's $t = 10.85$, $n = 15$, $df = 28$, $P < 0.0005$). Therefore, a reduction in *fli I* function, which presumably inhibits contraction, can partially suppress IFM collapse in *canB2* mutants.

canB2 shows a genetic interaction with an antimorphic allele of mhc

Some mutations in the *mhc* gene cause collapse of the IFM due to hypercontraction (Kronert et al., 1995), making it an attractive candidate for a target of calcineurin regulation. To test for the possibility of a genetic interaction between *canB2* and *mhc*, flies heterozygous for *canB2[EP(2)0774]* and *Mhc[5]*, a myosin allele that causes hypercontraction, were crossed, and serial sections of the thoraces of the transheterozygous offspring examined. Flies were scored as normal if all the IFM were in their proper positions and of normal size throughout the sections (Fig. 3A), mildly defective if a few of the sections displayed missing or abnormally shaped muscles (Fig. 3B), or if there were problems with DLM template splitting, and severely defective if most of the sections showed missing or abnormally shaped muscles (Fig. 3C). The lesion responsible for the *Mhc[5]* mutation is a change from glycine to aspartate at amino acid position 200 within exon 4, which disrupts the ATPase domain. In genetic tests it behaves as an antimorph. The addition of extra wild type Mhc alleles cannot completely suppress the hypercontractive phenotype (Homyk and Emerson, 1988). When heterozygous, the *Mhc[5]* mutation has a semi-dominant effect on the IFM; 55% of *Mhc[5]* heterozygotes examined had mild IFM defects, while 30% were severely affected. In contrast only 10% of the *Mhc[5]+/+ canB2[EP(2)0774]* flies had mild IFM defects, but the percentage of severe defects was increased to 80% (Fig. 3D) (Log-likelihood ratio: $G = 22.946$, $n = 20$, $df = 2$, $P < 0.001$). These results show that a decrease in calcineurin function enhances the dominant IFM phenotype of *Mhc[5].*

canB2 affects levels of mhc transcripts in the IFM

The results of the genetic test pointed to an interaction between *canB2* and *mhc*. Since alternative spicing controls *mhc* isoform production, we examined the expression of different isoforms in dissected IFM and whole abdominal tissue of wild type and *canB2* mutant flies, via RT-PCR, using equivalent

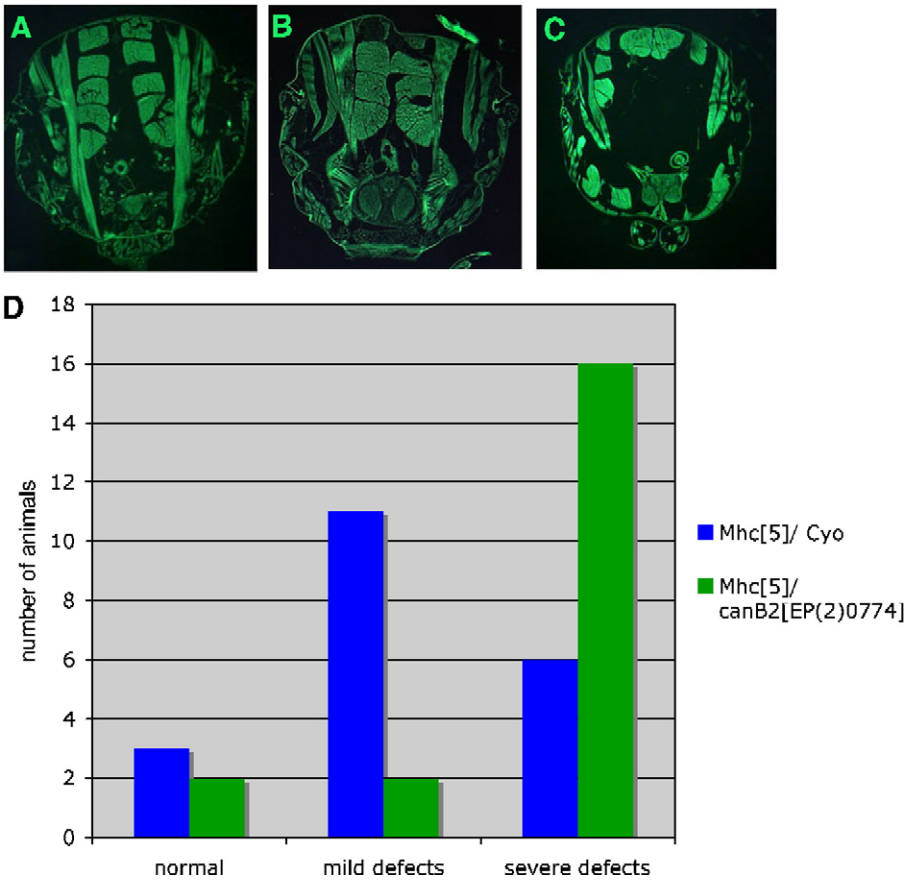

Fig. 3. One copy of the *canB2* mutation can enhance the muscle phenotype of the *Mhc[5]* mutation. (A) Cross section of the thorax of a *Mhc[5]/CyO* fly with a normal muscle phenotype. (B) Cross section of the thorax of a *Mhc[5]/CyO* fly with mild muscle defects. (C) Cross section of the thorax of a *Mhc[5]+/+ canB2[EP(2)0774]* fly with severe muscle defects. (D) Bar graph representation of the distribution of different muscle phenotypes of *Mhc[5]/CyO* (blue bars) and *Mhc[5]+/+ canB2[EP(2)0774]* (green bars) flies (n = 20).

amounts of flies. There are 5 different, mutually exclusive versions of *mhc* exon 11 (George et al., 1989; Fig. 4A); 11e is the only exon 11 variant found in the IFM, and it is expressed nowhere else (Hastings and Emerson, 1991). To test for the presence of each exon 11 variant, a primer for exon 2 (a common exon) and a primer for each version of exon 11 were used in separate PCR reactions, using equivalent numbers of flies. The 11e primer gives a strong band of the expected size (2.1 kb) in the wild type IFM, and is detectable in the mutant IFM only if 35 or more PCR cycles are used (Fig. 4B). When equivalent amounts of RNA (as opposed to equivalent numbers of flies) are used, the 11e-specific PCR product can be readily detected in *canB2* mutants, but at noticeably lower levels (data not shown). The mutant PCR product was cloned and sequenced, and was identical to the wild type cDNA sequence. None of the other exon 11 primers produced PCR products in either wild type or mutant cDNA from IFM. As a control, these primers were also tested on cDNA prepared from whole female abdomens, which contain body wall muscle, gut muscle, and muscle in the reproductive system (Fig. 4C). No bands were detected using the IFM-specific 11e primer in either WT or mutant abdominal cDNA. Bands were seen with both genotypes with the 11c and 11d primers, with the mutant bands noticeably weaker.

The levels of total myosin transcripts (in equivalent numbers of flies) were examined in the wild type and *canB2* mutants using primers from two common exons, 6 and 12 (Fig. 4A). In abdominal cDNA preparations (Fig. 4D) a band of the expected size (1.7 kb) was observed in both genotypes, with a slight decrease in the strength of the mutant band. In the IFM cDNA preparations, the wild type band (which would be exclusively the 11e isoform) is strong, while the equivalent band is not detectable in the mutant lane. Interestingly, the levels of GFP transcripts from the *mhc-GFP* reporter construct (Chen and Olson, 2001) used in our studies (Gajewski et al., 2003) are also greatly reduced in a *canB2* mutant background (data not shown), but not enough to completely abolish the presence of GFP protein.

RNA preparations done on equal numbers of wild type and *canB2* mutant flies showed that the mutants consistently had lower levels of total RNA (data not shown). To rule out a non-specific suppression of transcription as the cause of *mhc* transcript level reduction in the *canB2* mutants, we also examined the expression of the IFM expressed *88Factin* (Fig. 4E). A faint band was detectable in wild type abdominal cDNA, which agrees with reports of low levels of *actin88F* expression in the female ovary (Nongthomba et al., 2001). No such transcript was detected in the *canB2* abdominal cDNA. In the IFM preparations, both genotypes showed a strong band of the expected size (1.2 kb). This confirms that the reduction of *mhc* transcripts seen in *canB2* mutants is not due to an across the

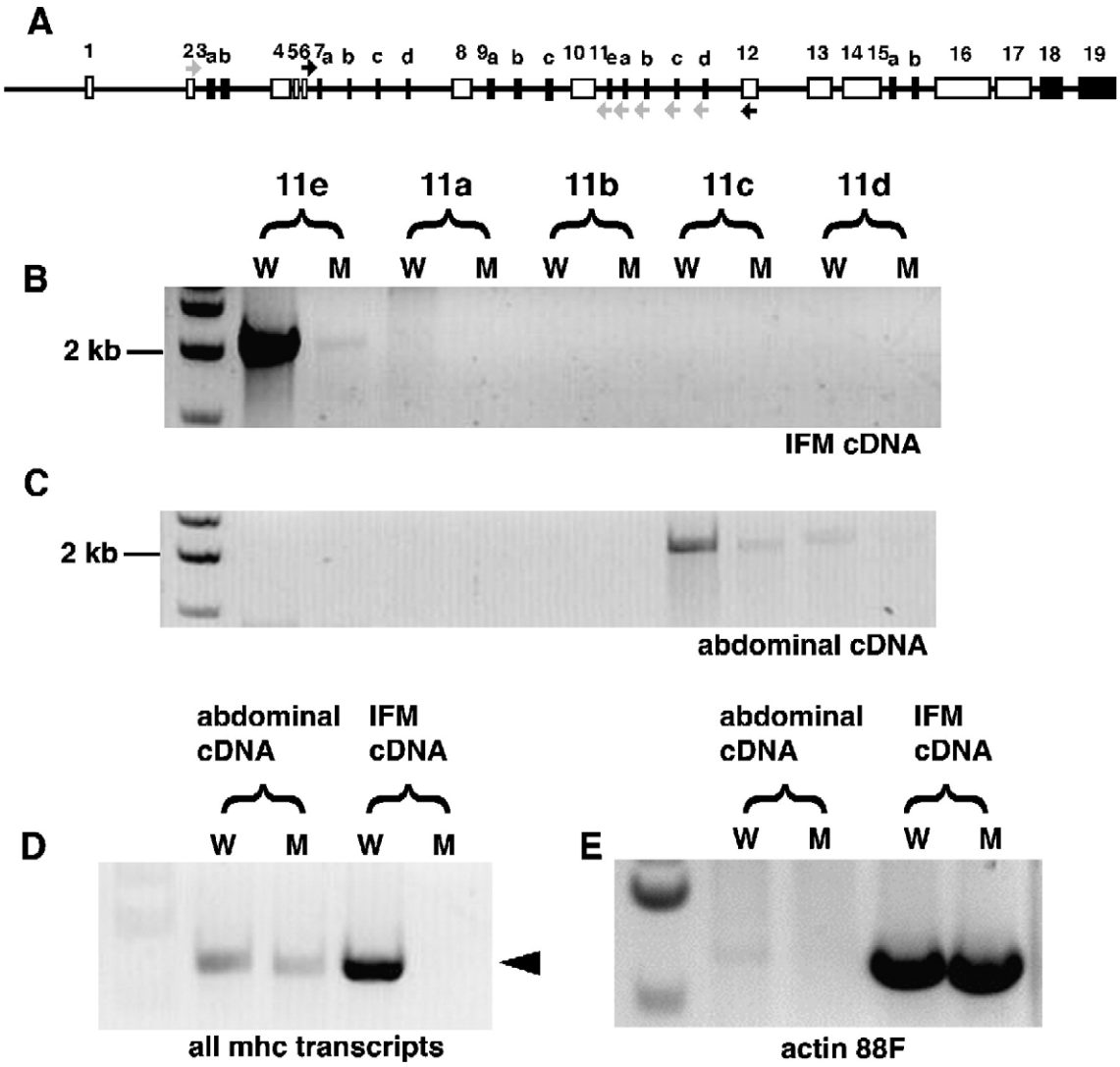

Fig. 4. Reduction of *mhc* transcripts in the IFM of *canB2* mutants. (A) Map of the *mhc* gene (modified from Standiford et al., 1997a). Common exons are denoted by white boxes, alternative exons by black. Primers for exon 2 and the five exon 11 versions are indicated with grey arrows; primers for exons 6 and 12 with black arrows. (B) Gel of the RT-PCR reactions with IFM cDNA from adult wild type and *canB2* mutant flies, using primers from exon 2 and one of the exon 11 variants, and 35 PCR cycles. The far left lane is the size marker; W denotes wild type cDNA, M mutant cDNA, and the specific exon 11 primer used shown above each pair. (C) Gel of the RT-PCR reactions with cDNA from whole adult female abdomens, done under the same PCR conditions and denoted in the same manner as the experiment with the IFM cDNA. (D) Gel of the RT-PCR reactions using primers from exons 6 and 12, which amplify all *mhc* isoforms. (E) Gel of the RT-PCR reactions using actin 88F primers.

board decrease in transcription. Therefore, calcineurin function is required for proper levels of *mhc* transcripts, especially in the IFM, but plays no role in the tissue-specific splicing of this gene.

Myofibrillar phenotype of canB2 mutant flies

A cross-section of wild type adult myofibrils shows the hollow thick filaments typical of IFM, and the standard hexagonal arrangement of thick and thin filaments (Fig. 5A). *canB2* mutant tissues show a range of phenotypes. In about 20% of the adult mutant tissue examined, the myofibrils are identical in appearance to wild type (data not shown), but others (about 40%) have scattered patches of organized filament structure at the periphery, and the central regions have no discernable filament structure (Figs. 5B and C). The rest of the mutant myofibrils lack any recognizable structures. The phenotype of mutant pupal muscle was even more severe; there was no organized filament structure in any of the mutant cross sections examined (Fig. 5D). Longitudinal sections revealed similar variability in the mutants. The wild type samples showed the characteristic pattern of Z-bands and M-lines (Fig. 6A). A small portion of the mutant myofibrils was indistinguishable from the wild type (data not shown). In some mutant muscle, broken or abnormally short Z-bands were seen as well as missing or partial M-lines, indicative of an absence or reduction in thick filaments (Fig. 6B). In this sample (Fig. 6B), the length of the sarcomeres is noticeably shorter than the wild type (Fig. 6A), consistent with a hypercontracted phenotype. Mutant pupae again showed the strongest phenotypes. In the most severely affected muscles, no Z-bands or any other markers of sarcomeric structure were found (Fig. 6C). Therefore, most of the myofibrils of canB2 mutant flies have

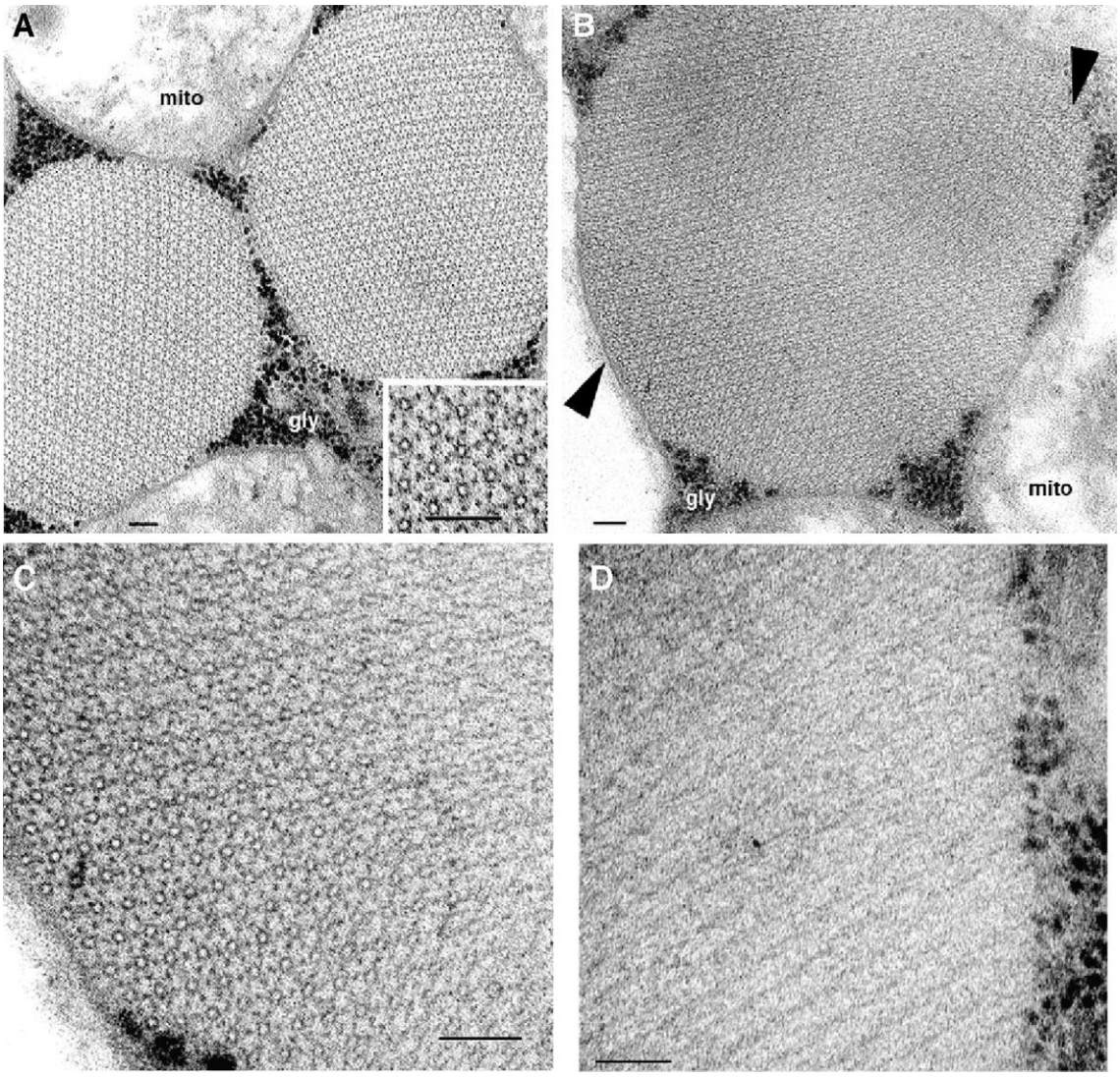

Fig. 5. Electron microscopy of wild type and *canB2* mutant IFM in cross section. (A) Two wild type adult myofibrils at 75,000×. The inset showing the details of filament structure is 200,000×. (B) Cross section of an adult *canB2* mutant myofibril at 75,000×. Arrowheads point to regions with discernable filament structure. (C) Close up of the bottom left portion of B, at 200,000×. (D) Myofibril of a "stage 3" *canB2* mutant pupa, at 200,000×. Bars are 100 nm. Mitochondria are denoted by "mito", glycogen granules by "gly".

reduced or absent thick filaments, which is an expected result of a severe reduction in *mhc* expression.

canB2 affects IFM-specific splicing of Tn I transcripts

Some mutants of *Tn I* are also known to cause hypercontraction and collapse of the IFM in the pupal or early adult stages (Beall and Fyrberg, 1991; Barbas et al., 1993; Kronert et al., 1999). To examine the state of *Tn I* transcripts in *canB2* mutants, we used PCR primers from two common exons, exon 2 and exon 5 (Fig. 7A), that span the IFM-specific exon 3; this allows for amplification of both splice forms of the *Tn I* transcript. For both wild type and mutant abdominal cDNA controls, the PCR product was 273 bp, the size expected if exon 3 were excluded (Fig. 7B). In the wild type IFM lane, there is a strong band at 456 bp (the size expected if exon 3 is included), and a barely detectable band at 273 bp. The mutant IFM result is the exact opposite, with a strong band at 273 bp, and weak band at 456 bp (Fig. 7B). The stronger bands of both genotypes were cloned and sequenced, and the sequences confirmed that the larger band includes *Tn I* exon 3, while the smaller band excludes it.

A reduction of the amount of the exon 3 containing *Tn I* isoform might present a possible explanation for the collapse of *canB2* mutant IFM. However recent work has shown that only the smaller, exon 3 lacking isoform is expressed during the early stages of IFM development. The larger isoform is detected much later, after 75 h APF (Nongthomba et al., 2004). To determine whether this isoform transition occurs at the transcriptional level before, during, or after the time of muscle collapse in *canB2* mutant pupae, *Tn I* transcripts from pupae at several different stages of muscle development were compared to those of wild type. Stage 1 is defined as the beginning of myofibrillogenesis, just after the shortening of the DLMs (Fig. 8A). Stage 2 represents the completion of the second elongation, but prior to when the collapse occurs in *can*

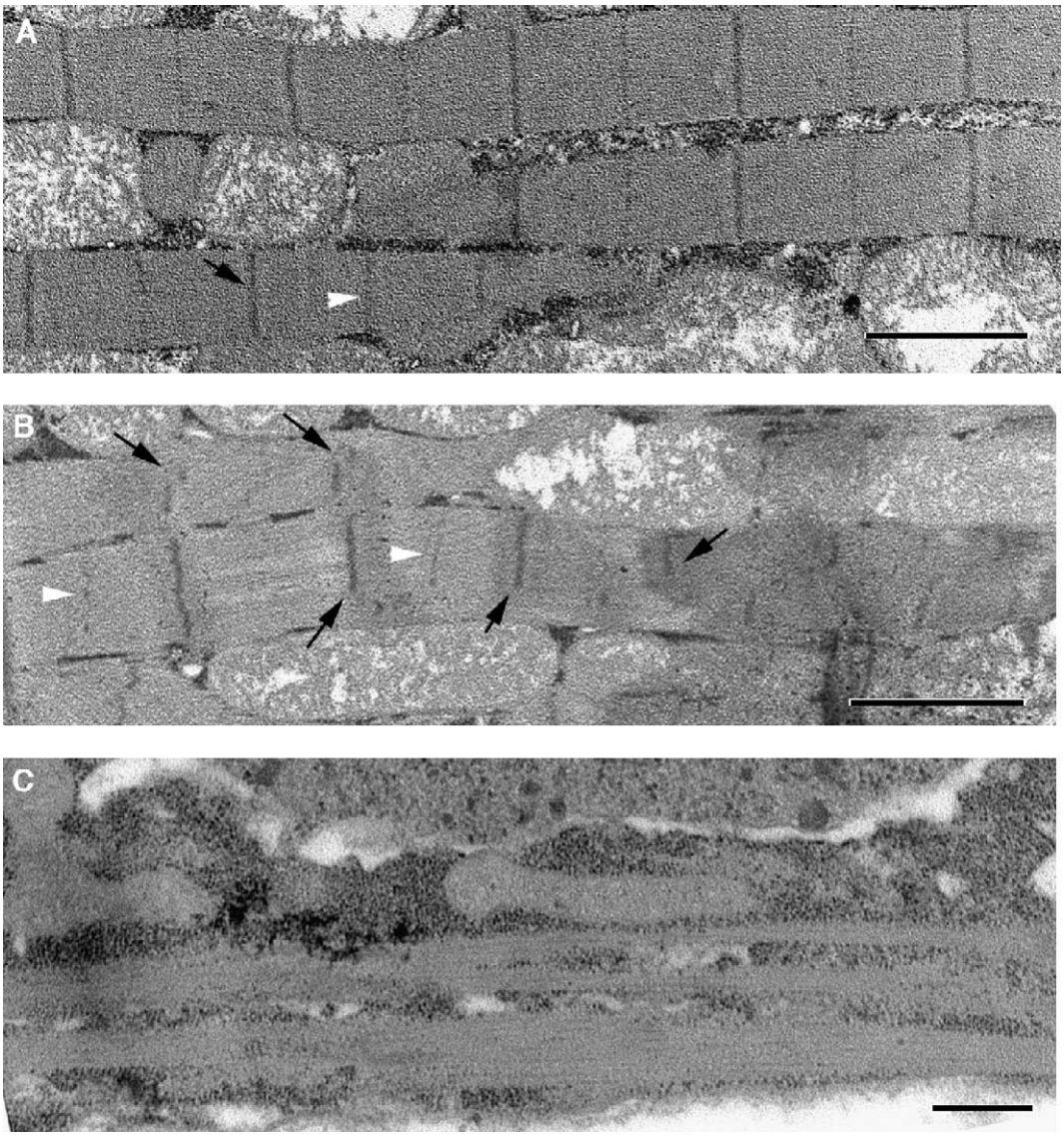

Fig. 6. Electron microscopy of wild type and *canB2* mutant IFM in longitudinal section. (A) Wild type myofibrils at 10,000×. The black arrow indicates a Z-band, the white arrowhead an M-line. (B) Myofibrils from an adult *canB2* mutant at 10,000×. Black arrows point to broken or abnormally short Z-bands, white arrowheads to partial M-lines. (C) Myofibrils from a "stage 3" *canB2* mutant pupa displaying the most severe phenotype observed, with no Z-bands or other sarcomeric markers, at 25,000×. The bars are 2 μm for A and B, 500 nm for C.

B2 mutants (Fig. 8B). Stage 3 is the point at which mutant muscles collapse, which happens before the first pigment is observed in the pupal eye (Fig. 8C). Comparison of the sizes of *Tn I* PCR products revealed that only the smaller, exon 3 minus form, is present in both the wild type and mutant IFM of all three pupal stages (Fig. 8D). Therefore, the failure of transition to the larger adult *Tn I* isoform cannot be a contributing factor in the collapse of the IFM in *canB2* mutants, as the collapse happens before the transition. The wild type adult lane has only the larger transcript, but in this PCR run the adult *canB2* mutant clearly shows transcripts for both isoforms (Fig. 8D).

Discussion

In this report, we further characterize the IFM collapse phenotype of the *canB2[EP(2)0774]* mutation. Studies of mutations in other loci that produce IFM collapse revealed two major causes for the phenotype: change of cell fate in the adepithelial cells of the 3rd Instar lava, or hypercontraction of the IFM muscle fibers. In mutants that cause a change in cell fate, such as *vg[null]*, a change in muscle cell fate can be clearly demonstrated by the loss of IFM-specific markers, and the ectopic expression of DFM-specific markers (Bernard et al., 2003). No such changes are observed in *canB2* mutant IFM. Unlike *vg[null]* mutants, the *88Factin-GFP* reporter is expressed strongly in *canB2* mutants, even after collapse of the IFM. A DFM-specific marker, *gD1142.1-lacZ*, expressed in a subset of DFM, also showed no alteration of expression pattern in *canB2* mutants. The expression of these reporters in the expected places indicates proper fate determination for the precursor cells that form the DFM and IFM.

Disruption of the myofibrillar structure by mutation of the *fli I* locus partially suppressed the IFM collapse phenotype,

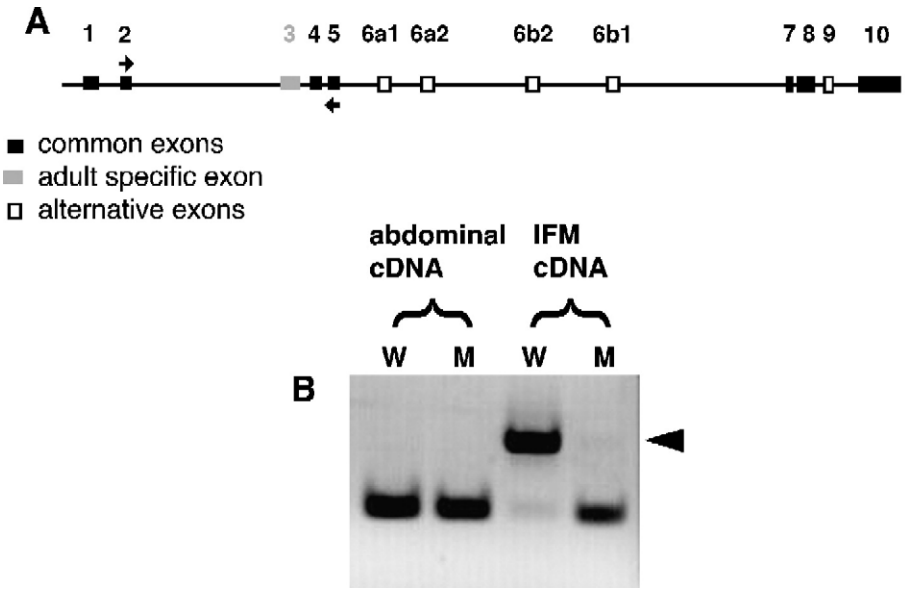

Fig. 7. *Troponin I* IFM-specific splicing is altered in *canB2* mutants. (A) Map of the *Tn I* gene. Common exons are denoted by black boxes, alternative exons with open boxes, and the adult-specific exon 3 in grey. Primers from exons 2 and 5 are indicated by the arrows. (B) Gel of RT-PCR reactions using the *Tn I* primers. Wild type lanes are indicated by W, mutant by M, and abdominal and IFM cDNA from adult flies by labeled brackets. An arrowhead points to the exon 3 containing isoform.

pointing to hypercontraction rather than a shift in cell fate as a cause. Addition of two doses of the *fli I[3]* allele to a *canB2* mutant background significantly increased the numbers of uncollapsed DLM. However, the suppression is not complete, and this may be due to the relatively mild effect of the *fli I[3]* allele. Null alleles of *fli I* cause lethality in the early embryonic stages. The *fli I[3]* allele is a less severe mutation, caused by a change of a highly conserved glycine to serine (de Couet et al., 1995). It is possible that even with the disruptions of the sarcomeric structure, *fli I[3]* does not completely inhibit IFM contraction.

A reduction of calcineurin function has a profound effect on the expression of the *mhc* gene in the IFM. One copy of *canB2[EP(2)0774]* enhances the severity of IFM defects in flies heterozygous for the antimorphic Mhc[5] allele. *mhc* transcripts are barely detectable in the IFM of *canB2* mutant flies, and many of the mutant myofibrils have greatly reduced or completely absent thick filaments. However, there is no interference with the tissue-specific splicing of the five versions of exon 11. The reduction of *mhc* expression is not due to a nonspecific reduction in transcription; the levels of GFP transcript from a reporter driven by *mhc* upstream sequences (*mhc-GFP*) are also reduced in a mutant background, but expression of actin88F is unaffected. The simplest explanation is that transcription of *mhc* is greatly reduced in the absence/reduction of calcineurin function, but further studies will be needed to confirm it.

The function of calcineurin in transcriptional activation is well documented, for example, its role in regulating transcription factors such as NFAT and Mef2. There are multiple Dmef2 binding sites upstream of the *mhc* gene, as well as a binding site for the zinc-finger transcription factor CF2 (Adams et al., 2000). Work in other systems has established that calcineurin can activate Mef2 both directly and indirectly; it is likely that it will also hold true for *Drosophila*. Whether calcineurin can affect CF2 activity is not yet known, but the phosphorylation state of CF2 has been demonstrated to play a role in its regulation via the EGFR pathway in *Drosophila* ovaries (Hsu et al., 1996; Mantrova and Hsu, 1998). Phosphorylated CF2 is found predominantly in the cytoplasm of the anterodorsal follicle cells, where it is fated to be degraded. It is speculated that removal of the phosphate group allows entry in the nucleus (Mantrova and Hsu, 1998). CF2 is expressed in all three muscle types of the *Drosophila* embryo (Bagni et al., 2002), but it is not yet known if this protein is required for IFM development. It will be of interest to investigate whether CF2 is expressed in the developing IFM, and what effects calcineurin function (or lack thereof) would possibly have on its subcellular localization.

It is also interesting to note that the lack/reduction of calcineurin has a much more drastic effect on *mhc* transcript levels in the IFM than it does on the various muscle types of the abdomen (Fig. 4D). The amount of total *mhc* transcripts are readily detectable in the mutant abdominal musculature, but not in the mutant IFM under the same PCR conditions. The transcript is not completely missing in the mutant IFM; if extra PCR cycles are done, or extra fly equivalents of cDNA are added for the mutants, a *mhc* band can be amplified. The reason for greater IFM sensitivity to lack of calcineurin function is unknown, and warrants further investigation. It may be that calcineurin is part of a system to promote maximum expression of *mhc*. The IFM are the largest muscles in the fly, and their tightly packed hexagonal arrangement of thick and thin filaments (unique in the fly musculature) could require increased expression of myosin and other structural proteins. There are numerous examples of mutations in muscle structural protein genes that result in a flightless phenotype, but do not impair the functions of other types of muscles (Fyrberg and Beall, 1990).

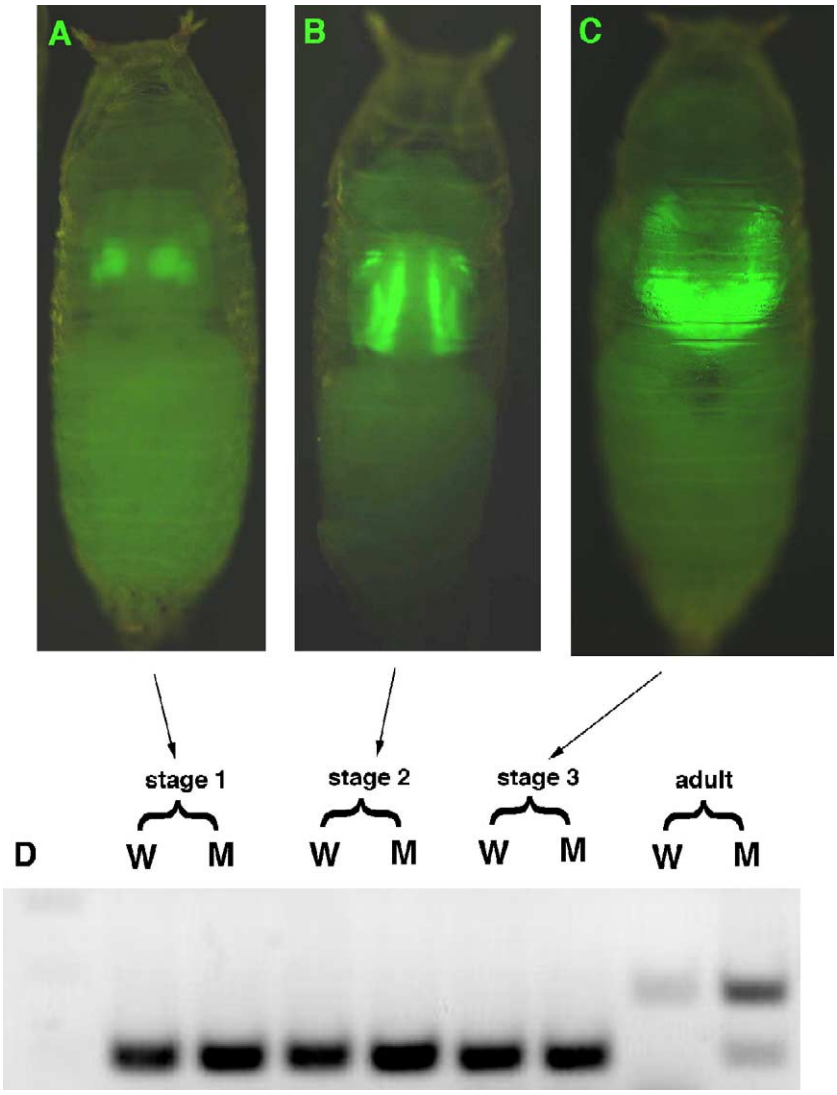

Fig. 8. The transition to the exon 3 containing *Tn I* splice form happens after the time of IFM collapse in *canB2* mutants. Animals in panels A to C express the *88Factin-GFP* reporter. (A) Example of a *canB2* mutant pupa at "stage 1". (B) Example of a wild type pupa at "stage 2". (C) Example of a *canB2* mutant pupa at "stage 3", the point of IFM collapse. (D) Gel of RT-PCR reactions of cDNA made from the IFM of wild type (W) and *canB2* mutant pupae (M) of the indicated stages, and from eclosed adult flies.

The myofilament structure of the *canB2* mutants reflects the reduction in *mhc* transcripts. While about 20% of the adult mutant IFM tissue examined resembled wild type, the majority of samples exhibited some degree of defect. Some myofibrils had patches of organized filament structure at the periphery, but had no recognizable structures in focus at the center region (Figs. 5B and C). This is likely the result of hypercontraction, which can lead to random myofilament orientation (Kronert et al., 1995). In the most severely affected myofibrils, no organized structures of any sort could be detected (Fig. 5D). Examination of longitudinal sections confirmed this range of phenotypes. Some samples resembled the wild type sarcomeric pattern. Mildly affected mutant tissue (Fig. 6B) had broken Z-bands, partial or missing M-lines (indicative of reduced or missing thick filaments), and shorter sarcomeres (indicative of hypercontraction). The most severely affected mutant muscles (Fig. 6C) lacked any Z-bands or M-lines. The mutant pupal samples tended to display the most severe myofibrillar phenotypes. It is likely that using adults for examination selects against the most severe phenotypes; the animals we examined in the pupal stage are likely to represent those that would not have successfully eclosed, and a small sample of *canB2* mutant pupae could easily display a propensity for the strongest defects. The *canB2[EP(2)0774]* mutation is semi-lethal; life cycle analysis reveals that many of the animals that die do so in the pupal stages (KG and RAS, unpublished observations). It may be that the most severe *canB2* phenotypes render the animals unable to eclose, although the role, if any, of the IFM is this process is yet to be confirmed. It is also possible that the most severe *canB2* phenotypes could impair other muscles.

The effect of the *canB2* mutation on Tn I expression represents a possible novel role for calcineurin, that being in different isoform formation. Although no direct role for calcineurin in the control of RNA splicing has yet been demonstrated, it is interesting to note that phosphorylation

status of SR proteins plays a role in their localization within the nucleus, and assembly, disassembly, and activity of the spliceosome may by influenced by a cycle of protein phosphorylation (reviewed in Misteli and Spector, 1997). The degree of phosphorylation is believed to effect protein–protein and protein–RNA interactions in the spliceosomal complexes (Mermoud et al., 1994; Cao et al., 1997; Tacke et al., 1997). In *Drosophila*, the splicing regulators *transformer* and *transformer2*, which function to splice doublesex pre-mRNA in a female-specific fashion, are highly phosphorylated (Du et al., 1998). The splicing of at least one variant exon of the mouse CD44 gene is coupled to signal transduction via the protein kinase C/ras signaling pathway (Konig et al., 1998). Therefore, it is possible that calcineurin helps regulate a system responsible for transition in the pupal IFM from the smaller Tn I isoform to the larger version, by control of the phosphorylation states of one or more proteins in the spliceosome complex that are required for inclusion of the third exon.

It should be noted that the effects of the *canB2* mutation on the relative levels of the two *Tn I* isoforms in the adult IFM are highly variable. In some PCR experiments, the smaller, exon 3 lacking transcript is predominant (Fig. 6B), but in others, both forms can be clearly seen (Fig. 7D). However, the results for the wild type adults are consistent: the larger transcript is clearly present, with little or no smaller form detected, in multiple repeats of the experiment. Thus, it must be considered that the differential formation of the *Tn I* isoforms may not be a direct result of altered calcineurin control of splicing in the IFM, but an indirect consequence of the physiological status of mutant versus normal muscle. That is, the switch to the larger exon 3 containing isoform may normally occur in a wild type genetic background due to some signal (or muscle state) perceived and transmitted within IFM that is of a proper developmental age and competency. In *canB2* mutants, an abnormal cellular environment may exist in some or all IFM that prevents the normal sensing of this signal and subsequent isoform switch. Thus, the variability we observe in the relative ratio of the two *Tn I* mRNA forms may simply reflect a nonequivalent status of collapsed muscles as to their competency to sense and execute this developmental molecular switch.

Taken together, our results have provided mechanistic insights into the cause of IFM collapse in *canB2* mutants. Cell fate changes can be ruled out, as can problems with *mhc* isoform production. In *canB2* mutants, the transition to the adult *Tn I* splice variant is incomplete at best, but this change occurs after the time when the muscles collapse, so an altered stoichiometry of troponin isoforms cannot contribute to this phenotype. Reduction of calcineurin function in the IFM leads to lower levels of *mhc* transcripts and a variable reduction in the numbers of thick filaments. This reduction in *mhc* expression is likely a major contributing factor in the collapse of the *canB2* mutant IFM. Heterozygotes of *Mhc[1]*, which is a null allele, have reduced numbers of thick filaments and partial hypercontraction of the IFM (Nongthomba and Ramachandra, 1999). However, there is a striking difference in the collapse phenotypes of *canB2* and various *mhc* mutations. In *canB2* mutants, without fail, the collapse of the IFMs is directed towards the posterior of the thorax. In a number of different *mhc* mutant alleles, the IFM can bunch to either side of the thorax (Kronert et al., 1995; Nongthomba et al., 2003; Montana and Littleton, 2004). The most severe myofibrillar phenotypes also suggest problems with more than just *mhc*. The strongest *canB2* phenotypes had no Z-bands or any semblance of sarcomeric structure, an effect seen in some mutations that cause defects in the thin filaments (Sparrow et al., 1991; Nongthomba et al., 2004). In animals homozygous for the *Tn I* allele *heldup[3]* (*hdp[3]*), which is functionally a null in the IFM, pupal myofibrils showed diffuse Z-bands at 42 h APF, and no sarcomeric structures by 46–48 h APF (Nongthomba et al., 2004). Since we see no Z-bands in the most severely affected *canB2* mutant pupae (at a later stage), it is possible that Z-bands could form and break down in a manner similar to *hdp[3]* mutants. Therefore, it is quite likely that expression and/or processing of other muscle structural proteins are regulated by calcineurin activity, and these warrant future investigation.

Acknowledgments

We would like to thank S. Bernstein and D. Standiford for providing us with fly stocks, R. Cripps for opinions on data, T. Felton and K. Dunner for technical assistance, J. Vincentz, D. Needleman, and M. Newhouse for technical advice, and L. McCord for assistance with figures. DNA sequences were determined by the M.D. Anderson Sequencing Facility, supported by NIH grant CA16672. Electron microscopy was performed by the MD Anderson Electron Microscope Core, supported by NIH Grant CA16672. This research was funded by grants to RAS from the NIH and Muscular Dystrophy Association. KG was supported by an American Heart Association Scientist Development Grant.

References

Adams, M.D., 2000. The genomic sequence of *Drosophila melanogaster*. Science 287, 2185–2195.

Barbas, J.A., Galceran, J., Torroja, L., Prado, A., Ferrus, A., 1993. Abnormal muscle development in the heldup3 mutant of *Drosophila melanogaster* is caused by a splicing defect affecting selected Troponin I isoforms. Mol. Cell. Biol. 13, 1433–1439.

Bagni, C., Bray, S., Gogos, J., Kafatos, F.C., Hsu, T., 2002. The *Drosophila* zinc finger transcription factor CF2 is a myogenic marker downstream of MEF2 during muscle development. Mech. Dev. 117, 265–268.

Beall, C.J., Fyrberg, E., 1991. Muscle abnormalities in *Drosophila melanogaster heldup* mutants are caused by missing or aberrant Troponin-I isoforms. J. Cell Biol. 114, 941–951.

Bernard, F., Lalouette, A., Gullard, M., Jeantet, A.Y., Cossard, R., Zider, A., Ferveur, J.F., Silber, J., 2003. Control of *apterous* by *vestigial* drives indirect flight muscle development in *Drosophila*. Dev. Biol. 260, 391–403.

Bernstein, S.I., O'Donnell, P.T., Cripps, R.M., 1993. Molecular genetic analysis of muscle development, structure, and function in *Drosophila*. Int. Rev. Cytol. 143, 63–151.

Cao, W., Jamison, S.F., Garcia-Blanco, M.A., 1997. Both phosphorylation and dephosphorylation of ASF/SF2 are required for pre-mRNA splicing in vitro. RNA 3, 1456–1467.

Chen, E.H., Olson, E.N., 2001. Antisocial, an intracellular adaptor protein, is required for myoblast fusion in *Drosophila*. Dev. Cell 1, 705–715.

Chin, E.R., Olson, E.N., Richardson, J.A., Yang, Q., Humphries, C., Shelton, J.M., Wu, H., Zhu, W., Bassel-Duby, R., Williams, R.S., 1998. A calcineurin-dependent transcriptional pathway controls skeletal muscle fiber type. Genes Dev. 12, 2499–2509.

de Couet, H.G., Fong, K.S., Weeds, A.G., McLaughlin, P.J., Miklos, G.L., 1995. Molecular and mutational analysis of a gelsolin-family member encoded by the *flightless I* gene of *Drosophila melanogaster*. Genetics 141, 1049–1059.

Du, C., McGuffin, M.E., Dauwalder, B., Rabinow, L., Mattox, W., 1998. Protein phosphorylation plays an essential role in the regulation of alternative splicing and sex determination in *Drosophila*. Mol. Cell 2, 741–750.

Dunn, S.E., Burns, J.L., Michel, R.N., 1999. Calcineurin is required for skeletal muscle hypertrophy. J. Biol. Chem. 274, 21908–21912.

Fernandez, J., Bate, M., Vijayraghaven, K., 1991. Development of the indirect flight muscles of *Drosophila*. Development 113, 67–77.

Flanagan, W.H., Corthesy, B., Bram, R.J., Crabtree, G.R., 1991. Nuclear association of a T-cell transcription factor blocked by FK-506 and cyclosporine A. Nature 352, 803–807.

Friday, B.B., Mitchell, P.O., Kegley, K.M., Pavlath, G.K., 2003. Calcineurin initiates skeletal muscle differentiation by activating MEF2 and MyoD. Differentiation 71, 217–227.

Fujita, S.C., Inoue, H., Yoshioka, T., Hotta, Y., 1987. Quantitative tissue isolation from *Drosophila* freeze-dried in acetone. Biochem. J. 243, 97–104.

Fyrberg, E., Beall, C., 1990. Genetic approaches to myofibril form and function in *Drosophila*. Trends Genet. 6, 126–131.

Gajewski, K., Wang, J., Molkentin, J., Chen, E.H., Olson, E.N., Schulz, R.A., 2003. Requirement of the calcineurin subunit gene *canB2* for indirect flight muscle formation in *Drosophila*. Proc. Natl. Acad. Sci. U. S. A. 100, 1040–1045.

George, E.L., Ober, M.B., Emerson, C.P., 1989. Functional domains of the *Drosophila melanogaster* muscle myosin heavy-chain gene are encoded by alternatively spliced exons. Mol. Cell. Biol. 9, 2957–2974.

Hastings, G.A., Emerson, C.P., 1991. Myosin functional domains encoded by alternative exons are expressed in specific thoracic muscles of *Drosophila*. J. Cell Biol. 114, 263–276.

Homyk, T., Emerson, C.P., 1988. Functional interactions between unlinked muscle genes within haploinsufficient regions of the *Drosophila* genome. Genetics 119, 105–121.

Hsu, T.C., Bagni, C., Sutherland, J.D., Kafatos, F.C., 1996. The transcription factor CF2 is a mediator of EGF-R-activated dorsoventral patterning in *Drosophila* oogenesis. Genes Dev. 10, 1411–1421.

Konig, H., Ponta, H., Herrlich, P., 1998. Coupling of signal transduction to alternative pre-mRNA splicing by a composite splice regulator. EMBO J. 17, 2904–2913.

Kronert, W.A., O'Donnell, P.T., Fieck, A., Lawn, A., Vigoreaux, J.O., Sparrow, J.C., Bernstein, S.I., 1995. Defects in the *Drosophila* myosin rod permit sarcomere assembly but cause flight muscle degeneration. J. Mol. Biol. 249, 111–125.

Kronert, W.A., Acebes, A., Ferrus, A., Bernstein, S.I., 1999. Specific myosin heavy chain mutations suppress *troponin I* defects in *Drosophila* muscles. J. Cell Biol. 144, 989–1000.

Liu, J., Farmer Jr., J.D., Lane, W.S., Friedman, J., Weissman, I., Schreiber, S.L., 1991. Calcineurin is a common target of cyclophilin–cyclosporin A and FKBP–FK506 complexes. Cell 66, 807–815.

Lyons, G.E., Schiaffino, S., Sassoon, D., Barton, P., Buckingham, M., 1990. Developmental regulation of myosin gene expression in mouse cardiac muscle. J. Cell Biol. 111, 2427–2436.

Mantrova, E.Y., Hsu, T., 1998. Down-regulation of transcription factor CF2 by *Drosophila* Ras/MAP kinase signaling in oogenesis: cytoplasmic retention and degradation. Genes Dev. 12, 1166–1175.

Mermoud, J.E., Cohen, P.T.W., Lamond, A.I., 1994. Regulation of mammalian spliceosome assembly by a protein phosphorylation mechanism. EMBO J. 13, 5679–5688.

Miklos, G.L., De Couet, H.G., 1990. The mutations previously designated as *flightless-I3, flightless-O2* and *standby* are members of the W-2 lethal complementation group at the base of the X-chromosome of *Drosophila melanogaster*. J. Neurogenet. 6, 133–151.

Misteli, T., Spector, D.L., 1997. Protein phosphorylation and the nuclear organization of pre-mRNA splicing. Trends Cell Biol. 7, 135–138.

Montana, E.S., Littleton, J.T., 2004. Characterization of a hypercontraction-induced myopathy in *Drosophila* caused by mutations in Mhc. J. Cell Biol. 164, 1045–1054.

Nongthomba, U., Ramachandra, N.B., 1999. A direct screen identifies new flight muscle mutants on the *Drosophila* second chromosome. Genetics 153, 261–274.

Nongthomba, U., Clayton, J.J., Pasalodos-Sanchez, S., Sparrow, J.C., 2001. Expression and function of the *Drosophila* ACT88F actin isoform is not restricted to the indirect flight muscles. J. Muscle Res. Cell Motil. 22, 111–119.

Nongthomba, U., Cummins, M., Clark, S., Vigoreaux, J.O., Sparrow, J.C., 2003. Suppression of muscle hypercontraction by mutations in the myosin heavy chain gene of *Drosophila melanogaster*. Genetics 164, 209–222.

Nongthomba, U., Clark, S., Cummins, M., Ansari, M., Stark, M., Sparrow, J.C., 2004. Troponin I is required for myofibrillogenesis and sarcomere formation in *Drosophila* flight muscle. J. Cell Sci. 117, 1795–1805.

Peckham, M., Moloy, J.E., Sparrow, J.C., White, D.C.S., 1990. Physiological properties of the dorsal longitudinal flight muscle and the tergal depressor trochanter muscle of *Drosophila*. J. Muscle Res. Cell Motil. 11, 203–215.

Rivlin, P.K., Schneiderman, A.M., Booker, R., 2000. Imaginal pioneers prefigure the formation of adult thoracic muscles in *Drosophila melanogaster*. Dev. Biol. 222, 450–459.

Schiaffino, S., Reggiani, C., 1996. Molecular diversity of myofibrillar proteins: gene regulation and functional significance. Physiol. Rev. 76, 371–423.

Schulz, R.A., Yutzey, K.E., 2004. Calcineurin signaling and NFAT activation in cardiovascular and skeletal muscle development. Dev. Biol. 266, 1–16.

Sparrow, J., Reedy, M., Ball, E., Kyrtatas, V., Molloy, J., Durston, J., Hennessey, E., White, D., 1991. Functional and ultrastructural effects of a missense mutation in the indirect flight muscle-specific actin gene of *Drosophila melanogaster*. J. Mol. Biol. 222, 963–982.

Standiford, D.M., Davis, M.B., Sun, W., Emerson, C.P., 1997a. Splice-junction elements and intronic sequences regulate alternative splicing of the *Drosophila* myosin heavy chain gene transcript. Genetics 147, 725–741.

Standiford, D.M., Davis, M.B., Miedema, K., Franzini-Armstrong, C., Emerson, C.P., 1997b. Myosin rod protein: a novel thick filament component of *Drosophila* muscle. J. Mol. Biol. 265, 40–55.

Sudarsan, V., Anant, S., Guptan, P., VijayRaghaven, K., Skaer, H., 2001. Myoblast diversification and ectodermal signaling in *Drosophila*. Dev. Cell 1, 829–839.

Tacke, R., Chen, Y., Manley, J.L., 1997. Sequence-specific RNA binding by an SR protein requires RS domain phosphorylation: creation of an Srp40-specific splicing enhancer. Proc. Natl. Acad. Sci. U. S. A. 94, 1148–1153.

Wu, H., Rothermel, B., Kanatous, S., Rosenberg, P., Naya, F.J., Shelton, J.M., Hutchenson, K.A., DiMaio, J.M., Olson, E.N., Bassel-Duby, R., Williams, R.S., 2001. Activation of MEF2 by muscle activity is mediated through a calcineurin-dependent pathway. EMBO J. 20, 6414–6423.

Zhang, C.L., McKinsey, T.A., Chang, S., Antos, C.L., Hill, J.A., Olson, E.N., 2002. Class II histone deacetylases act as signal-responsive repressors of cardiac hypertrophy. Cell 110, 479–488.